NASA Technical Paper 1201

Effect of Anode-Cathode Geometry on Performance of the HIP-1 Hot Ion Plasma

Milton R. Lauver

APRIL 1978

NASA

NASA Technical Paper 1201

Effect of Anode-Cathode Geometry on Performance of the HIP-1 Hot Ion Plasma

Milton R. Lauver
Lewis Research Center
Cleveland, Ohio

NASA
National Aeronautics
and Space Administration

Scientific and Technical Information Office

1978

EFFECT OF ANODE-CATHODE GEOMETRY ON PERFORMANCE OF THE HIP-1 HOT ION PLASMA

by Milton R. Lauver

Lewis Research Center

SUMMARY

Additional results of hot-ion hydrogen plasma experiments conducted in the NASA Lewis HIP-1 magnetic mirror facility are presented. A steady-state $\underline{E}\times\underline{B}$ plasma was formed by applying a strong radially inward direct-current (dc) electric field near the throats of the magnetic mirrors. The dc electric field was created between opposed pairs of hollow cathode rods inside hollow anode cylinders, which were concentric with the magnetic axis. The purpose of these experiments was to determine how the ion temperature and the product of electron and neutral densities were influenced by the axial position of the cathode tips relative to the anodes.

The highest ion temperatures were attained when the tip of each cathode was in the same plane as the end of its anode. At this position steady-state hydrogen plasmas with ion temperatures of 900 eV were attained. This is 200 eV higher than the temperatures measured with the cathodes withdrawn 8 centimeters, to the position used for previous reports. These temperatures were reached with 22 kilovolts applied to the electrodes in a midplane field of 1.1 teslas. For the same current at a given voltage, the hydrogen flow input rate was reduced about 30 percent by moving the cathodes from the withdrawn position to the position coplanar with the anodes.

Scaling relations were empirically determined for ion temperature, and the product of ion density and neutral particle density as a function of cathode voltage, discharge current, and electrode positions. Plasma discharge current as a function of voltage (I-V) characteristics were determined.

INTRODUCTION

This report presents further results of the hot-ion hydrogen plasma experiments

---

*Presented in part at the International Conference on Plasma Science sponsored by the Institute of Electrical and Electronic Engineers, Austin, Texas, May 24-26, 1976.

conducted in the HIP-1 (Hot-Ion Plasma) facility at the NASA Lewis Research Center (refs. 1 to 3). HIP-1 is a water-cooled magnetic mirror facility with a mirror ratio of 1.82 and maximum magnetic flux density of 2.15 tesla at the mirrors. A steady-state plasma was formed by applying a radially inward direct-current electric field of several kilowatts per centimeter near the mirror throats. The mutually perpendicular electric and magnetic fields caused the plasma to rotate (drift) in the azimuthal direction. This azimuthal drift provided a kinetic energy input, largely to the ions. Randomization of this energy and enhancement of ion heating might have been due primarily to oscillations (refs. 4 and 5). This plasma heating process has been used in SUMMA (Superconducting Magnetic Mirror Apparatus at Lewis (refs. 6 and 7) and HIP-1 to produce ion temperatures up to several hundred electron volts for hydrogen plasmas.

In the evolution of HIP-1 (and SUMMA), uncooled cathode rods in long, uncooled cylindrical anodes have been replaced by larger water-cooled cathode rods in short water-cooled anodes (refs. 6 and 8). It was reported (ref. 3) that the optimum operating position for uncooled electrodes had the tip of the cathode rod withdrawn about 7.6 centimeters from the apparatus midplane end of its anode cylinder. This relationship continued to be used after the uncooled electrodes had been replaced by water-cooled ones and the anodes had been shortened. In the present report the axial positions of the cathodes relative to the anodes were varied to determine their effect on the plasma ion temperature, the product of neutral and electron densities, and I-V characteristics. The use of extensive water cooling permitted data gathering for minutes at a time under steady-state conditions.

The principal diagnostic instrument was an optical monochromator, used to estimate ion temperatures and on a relative basis the product of the ion density and neutral density by Doppler broadening of the H_α line. The remotely controlled monochromator apparatus and the method of using the second moment of the H_α line profiles to determine ion temperature were reported in reference 9.

APPARATUS

The HIP-1 facility was constructed to develop a hot-ion plasma source for use in thermonuclear research. The magnets and test section are described briefly in reference 3.

Magnet

Two water-cooled copper solenoids that operate in a steady-state manner serve as mirror magnets. They produce a field of up to 1.13 tesla at the midplane of the test

section and up to 2.06 tesla at the mirrors (mirror ratio of 1.82). Steady-state fields of 1.18 tesla at the midplane and 2.15 tesla at the mirrors were limited to 5 to 10 seconds duration to avoid overheating the magnets.

Plasma Test Section

A schematic view of the plasma test section and magnet configuration is shown in figure 1. The test section is a water-cooled hollow cylinder made of type 304 stainless steel. Its inner diameter is 25 centimeters and it is 1.63 meters long. Diffusion pumps at each end of the test section evacuate it to a base pressure of about 7×10^{-5} pascals.

A quartz window at each end port of the test section provides a good view, with the aid of a mirror, of the plasma and electrodes. Quartz or borosilicate glass windows on the midplane ports provide access for the spectroscopic diagnostics and for direct visual observation of the plasma.

Facility Instrumentation

A schematic of the gas fuel system is given in figure 2. The flowmeters and a magnetically shielded ion gage on the test section have remote readouts in the control room. Variable leak valves were used with two pressure regulators to set the flow rates of hydrogen into the east and west hollow cathodes manually.

The electrode high-voltage schematic is given in figure 3. The two power supplies (rated individually for 10 kV at 10 A) operated in series up to 23 kilovolts. An on-off high-voltage vacuum switch and variable voltage controllers in the supply cabinets were operated remotely from the control room. Cathode currents were measured with floated ammeters. The anode currents were obtained by measuring the voltage across the one ohm grounding resistors.

Electrode Assembly

Figure 1 shows the location of the anodes, cathodes, and electrically floated shields. It also shows the magnetic-field configuration. Figure 4 shows the electrode dimensions and defines coordinate d, the cathode-tip position.

Figure 5 shows a typical electrode assembly. The cathodes used for this report had a single outside diameter. A magnetic-field-line plot is superimposed on the outlines of the electrodes and test section in figure 6. The anodes were located outside of

the magnet mirrors.

Figure 7 is a photograph of four configurations of water-cooled anodes that have been used in HIP-1. The third from the left, which was 5.1 centimeters long, was used for the results reported herein. Figure 8 is a view of an anode and cathode, showing their coaxial relation. Figure 9 is a cutaway view of the cathode used.

The cathode-to-anode axial spacing, d (fig. 4), was varied from 15.2 to -5.1 centimeters in the parametric study.

The electrode components were fabricated from copper and stainless steel. They were all water cooled. To minimize sputtering those surfaces exposed to energetic plasma were made of copper, which was coated with tungsten by a commercial plasma flame-spraying process.

PLASMA DIAGNOSTICS

Apparatus

Figure 10 shows the optical emission spectroscopy apparatus used to determine ion temperature and relative ion density (ref. 9). The monochromator viewed the plasma along a line-of-sight that was perpendicular to the magnet axis at the test section midplane. All of the data in this report were taken with the monochromator line-of-sight intersecting the centerline of the plasma so the quantity y in figure 10 was zero. The entrance slit of the monochromator corresponded to an emission source approximately 2 millimeters in the vertical direction and 26 millimeters parallel to the magnet axis.

Analysis

Figure 11 shows a typical H_α line profile taken in HIP-1 with the spectroscopy apparatus. There was an intense narrow component due to electronic excitation, Stark broadening, and Franck-Condon neutrals and a wide Doppler-broadened component. The wide component was assumed to be due primarily to simultaneous electronic excitation and charge exchange by the reaction (ref. 1)

$$H_f^+ + H_2 \rightarrow H_f(n \geq 3) + H_2^+ \qquad (1)$$

where the subscript f stands for "fast" and n is the principal quantum number. The emission spectra from H_f was Doppler broadened because the H_f has essentially the same velocity as H_f^+. Therefore, the H_f^+ ion temperature averaged across the midplane diameter could be obtained from the width (or second moment) of the wide component of

the H_α line. The ion temperatures were obtained by the methods described in reference 1, where it was assumed that reaction (1) predominates.

The area A under the H_α faired curve is a measure of the rate of production of the wide component photons (fig. 11). This rate was assumed to be proportional to $\bar{n}_o \bar{n}_i \langle \overline{\sigma_\alpha v_i} \rangle$, where the symbols are defined in the appendix. Thus for the wide component curve of figure 11,

$$A \propto \bar{n}_o \bar{n}_i \langle \overline{\sigma_\alpha v_i} \rangle$$

or

$$\bar{n}_o \bar{n}_i \propto \frac{A}{\langle \overline{\sigma_\alpha v_i} \rangle} \tag{2}$$

The quantity $\langle \sigma_\alpha v_i \rangle$ was assumed to depend only on H^+ ion temperature. The relationship, based on optical cross sections for reaction (1) is shown in figure 12.

Since the constant of proportionality was not known for equation (2), only relative values of the product $\bar{n}_o \bar{n}_i$ were obtained in this way.

DISCUSSION OF RESULTS

Current Versus Voltage Characteristics of Plasma Discharge

Figure 13 shows the two types of hydrogen current-voltage (I-V) discharge curves reported for the HIP-1 hot-ion plasma process (ref. 1). These curves are for water-cooled hollow cathodes in the 1.3-centimeter-long water-cooled anodes shown at the left in figure 7 with the cathode tips positioned at d = 8.3 centimeters (fig. 4). The lower curve in figure 13 was typical of operation at either low magnetic fields or low gas flow rates; the upper, at either high magnetic fields or high gas flow rates. Gas was fed through the hollow cathodes. With the gas flow rate and magnetic field strength held constant, cathode voltage was the independent variable and the resulting current was the dependent variable.

In the present work it was noted that the cathode currents were larger than the anode currents, sometimes nearly twice as large at high voltages and currents. This difference is believed due largely to parasitic current loss from the cathodes via the floating plates to the test section walls. For this reason anode currents were chosen as the better measure of useful input to the plasma, to correlate with the H_α line profile emission data.

As reported in reference 1, at low gas flow rates there was a smooth increase in

current as the voltage increased to its maximum. At higher gas flow rates increasing the voltage from zero caused the current to increase rapidly for a few kilovolts. This plasma regime is referred to as the low-resistance mode. With hydrogen in HIP-1, the plasma appeared visibly bright and diffuse throughout the test section in this mode. As the voltage was raised further, the plasma system became unstable, spontaneously switching into a second mode referred to as the high-resistance mode and back to the low-resistance mode again. The rate of switching increased with voltage until the high-resistance mode stayed in control. The high-resistance mode was characterized visually by a distinct cylindrical plasma glow between opposing electrodes and an annular halo at the midplane of the magnetic mirrors. In the high-resistance mode region of both curves of figure 13, the resistance increased with voltage such that the current remained almost constant.

In the present experiments with 5.1 centimeter anodes, in addition to I-V curves of the type given in figure 13, another type of I-V curve was found in which the resistance remained almost constant. From the onset of measurable current, the I-V curve displayed an almost continuous linear increase in current as the voltage increased to its maximum. This occurred when the gas flow was relatively high and the cathode-anode axial distance d was 5.1 centimeters or less. A typical curve of this sort is shown in figure 14. When the distance d was as large as the 8.3 centimeters used in reference 1, the I-V curves were similar to those of figure 13. Like the high-resistance mode, this constant resistance mode was characterized by a distinct cylindrical glow between opposing electrodes and an annular midplane halo.

High ion temperatures were attained when the plasma was either in the high-resistance or constant-resistance mode, and low temperatures in the low-resistance mode.

High ion temperatures were always accompanied by a midplane halo like that shown in figure 15. The halo glow was probably due to ions with almost pure transverse velocities trapped in the minimum-B portion of the magnetic field. Some of these fast trapped ions charge exchange with the pervasive neutral background particles and fan out as fast neutrals in the midplane. Physical evidence supporting this concept could be found on the midplane windows. Although the quartz windows in the midplane viewing-port became coated with a layer of metal sputtered from the test section walls, a clear uncoated vertical stripe about 3 centimeters wide always remained, as a photograph shows (fig. 16). The window is about 36 centimeters from the magnetic axis (plasma beam).

Functional Dependence of Ion Temperature on Plasma Variables and Electrode Geometry

In this experiment the independent variables were gas flow rate G, magnetic field

B, cathode voltage V, and electrode geometry. Dependent variables are ion temperature T_i, ion density n_i, neutral density n_o, anode current I_a, cathode current I_c, electron temperature T_e, electric field E, plasma azimuthal drift velocity, stray electric currents, percent dissociation, etc. The values of most of the dependent variables depended on their location within the test section. The only dependent variable that could be directly measured (without data reduction) is the current.

Current, voltage, gas flow rate, and electrode geometry are plasma parameters that relate closely to experimental hardware limits. Current is a dependent variable that was conveniently and accurately measured. The ion temperature and $n_o n_i$ product are also dependent variables.

The 51 data points for which B = 1.08 to 1.09 tesla and d varied from 0 to 15.2 centimeters were analyzed with a linear regression program, which gave goodness of fit measures for the resulting equation and measures of confidence for the individual exponents. The program was used to get triple correlations of the form

$$Y = 10^{b_0} X_1^{b_1} X_2^{b_2} X_3^{b_3}$$

The data, presented in table I, gave a good fit to the equations

$$\left.\begin{aligned} T_i &= 10^{1.41}(d + 7.6)^{-0.39} I^{0.22} V^{1.43} \\ R^2 &= 0.97 \qquad F = 498 \qquad T_1 = 14 \qquad T_2 = 9.7 \qquad T_3 = 30 \end{aligned}\right\} \tag{3}$$

and

$$\left.\begin{aligned} T_i &= 10^{2.26}(d + 7.6)^{-0.99} G^{1.16} V^{1.52} \\ R^2 &= 0.96 \qquad F = 348 \qquad T_1 = 13 \qquad T_2 = 25 \qquad T_3 = 7 \end{aligned}\right\} \tag{4}$$

The large values of R^2 and F indicate an excellent fit of the data points to the equations. (See the appendix.) Figure 17 displays the correlation of the data with equation (3) on a rectilinear plot.

The values of T indicate that high confidence is justified in the accuracy of all three exponents, b_1, b_2, and b_3.

The exponents on $d + 7.6$ and V are different in equations (3) and (4). This is expected because the current is known to be a function of electrode geometry, gas flow rate, and voltage.

Reference 1 had reported the simple and approximate scaling relations for a fixed

value of B:

$$T_i \propto I^{0.32} V^{1.4} \qquad \text{and} \qquad T_i \propto G^{1.5} V^{1.4}$$

In common with equations (3) and (4), the voltage exponent is about 1.4. The exponent on G is about five times that on I, albiet both values are somewhat larger in the earlier correlations. All in all, the older correlations are in agreement with the newer.

The effect of the exponents on the electrode geometry factor $d + 7.6$ was to increase the ion temperature as d approached 0, or, conversely, withdrawing the cathode from the anode resulted in lower temperatures.

When the cathode was inserted past the magnetic midplane end of the anode, $d < 0$, the data obtained did not fit the correlations of equations (3) and (4). Further, no satisfactory correlation equation could be found.

The reason that T_i increases as d is decreased is not obvious. A possible explanation is that reducing d results in a longer axial region of strong electric field in the annular gap between the anode and cathode. Because the ion heating is strongly influenced by $\underline{E} \times \underline{B}$ effects, it seems reasonable that a longer region of strong $\underline{E}$ would result in greater ion heating. When the cathode tip protrudes beyond the inboard face of the anode, the region of plasma formation at the tip of the hollow cathode is outside of the strongest electric field region. Therefore, it is not surprising that the ion temperature might drop off as d becomes negative.

Functional Dependence of the Product of Ion Density and Neutral Particle Density on Plasma Variables and Electrode Geometry

The LINREG program was used to correlate the data of table I to show the relation of $\bar{n}_o \bar{n}_i$ to plasma variables. The resulting correlations were at best only fair. The six data points for $d = 0$ did not fit into a correlation with the other 45 points. With the 45 points ($d \geq 2.5$ cm), the results were

$$\left.\begin{aligned} \bar{n}_o \bar{n}_i &\propto (d + 7.6)^{1.31} I^{0.88} V^{-3.44} \\ R^2 = 0.97 \qquad F = 482 \qquad T_1 &= 15 \qquad T_2 = 15 \qquad T_3 = 28 \end{aligned}\right\} \tag{5}$$

and

$$\left.\begin{aligned} \bar{n}_o\bar{n}_i &\propto (d + 7.6)^{-0.29} G^{3.47} V^{-3.28} \\ R^2 = 0.89 \qquad F = 111 \qquad T_1 &= 5 \qquad T_2 = 0.9 \qquad T_3 = 13 \end{aligned}\right\} \tag{6}$$

The fit to the data points was excellent for equation (5) and fair for equation (6). Figure 18 displays the correlation of the data with equation (5) on a rectilinear plot. The exponents of equation (5) are probably accurate, as is the voltage exponent of equation (6). The exponent on G is not to be trusted. Reference 1 had reported the simple and approximate scaling relations for fixed value of B:

$$\bar{n}_o\bar{n}_i \propto I^{0.7} V^{-3.1} \qquad \text{and} \qquad \bar{n}_o\bar{n}_i \propto G^{3.4} V^{-3.1}$$

In common with equations (5) and (6), the voltage exponent was about -3.1. The exponential dependence of I and G were reasonably close to the values found here.

The positive and negative exponents on (d + 7.6) for equations (5) and (6), respectively, need clarification. With I, G, V, and B fixed, equations (5) and (6) indicate that increasing d would increase $\bar{n}_o\bar{n}_i$ (eq. (5)) or decrease $\bar{n}_o\bar{n}_i$ (eq. (6)). The explanation lies in the observation that increasing d requires G to be increased to hold I constant or that, if G is held constant, I decreases; that is, I, G, V, and B cannot be held fixed if d changes.

As was the case with ion temperature, when the cathode was inserted past the midplane end of the anode, $d < 0$, the data taken did not fit the correlations of equations (5) and (6). No satisfactory correlation equation for these data could be found.

CONCLUDING REMARKS

A steady-state hot-ion plasma was produced and studied in the Lewis HIP-1 facility using water-cooled electrodes.

The new variable studied was an electrode geometry, specifically the distance between the tip of each cathode and its corresponding coaxial anode. Voltage and gas flow rate were varied, and the resulting ion temperatures and products of electron and neutral densities were obtained for a number of geometries.

Scaling relations were empirically obtained for the ion temperatures as functions of geometry, voltage, and current and as functions of geometry, voltage, and gas flow rate. Scaling relations for the relative product of ion density and neutral particle density were also obtained.

The ion temperature was maximized by placing the cathode tips approximately at the midplane face of the anodes. The ion temperature increased with current, gas flow,

and voltage at all of the axial cathode positions whose data could be correlated.

The product of the ion density and neutral density was confirmed to increase with current and gas flow rate, and decrease with increasing voltage (ref. 1). The dependence of this product on electrode geometry was not clear; the correlations of the data could not be summarized in any simple manner.

An average hydrogen ion temperature of 900 eV was measured when 22 kilovolts was applied to the electrodes at a midplane magnetic flux density field of 1.08 tesla with the inboard end of the cathode coplanar with the inboard end of the anode. Under the same conditions, except for the cathode in the withdrawn position used for previous reports, an ion temperature of 700 eV was measured. A 30 percent higher gas flow, resulting in a higher pressure in the test section, had been needed to reach the highest ion temperature at the cathode position used for previous reports (ref. 1).

In addition to confirming previously measured current-voltage characteristics, conditions were found in which the current increased approximately linearly with voltage at high voltages - a constant resistance mode.

Lewis Research Center,
National Aeronautics and Space Administration,
Cleveland, Ohio, December 19, 1977,
506-25.

APPENDIX - SYMBOLS

A area of wide component of spectral line plot (fig. 11)

B magnetic flux density on the magnetic axis at midplane, T

$\underline{B}$ magnetic flux density vector

b an exponent when used with numerical subscripts

d cathode axial coordinate referred to anode, cm (fig. 4)

$\underline{E}$ electric field vector referred to fixed axes

F a distribution indicative of confidence; ratio of mean square due to regression to mean square due to residual variation. A low value (generally of 2 or less) indicates a poor fit

G volume rate of flow of gas, std. cm^3/sec

I total electric current, A

n_i number density of H^+ ions

n_o number density of H_2 neutrals

R^2 proportion of total variation about mean Y accounted for by regression equation; ratio of sum of squares due to regression to total sum of squares

T test indicative of confidence in individual exponents; value of 3 or less indicates a lack of confidence in b exponents of this report; subscript number corresponding to b.

T_i ion temperature, eV

V anode-cathode voltage, kV

v velocity

σ cross section

Subscripts:

c charge exchange

f fast

i H^+ ion

o neutral or H_2

α atomic hydrogen Balmer α line

Special Symbols:

$\langle\ \rangle$ Maxwell-Boltzmann average of included quantity

$\bar{}$ radial average across the diameter at midplane

REFERENCES

1. Reinmann, J. J.; et al.: Hot Ion Plasma Production in HIP-1 Using Water-Cooled Hollow Cathodes. NASA TM X-71852, 1975.

2. Sigman, Donald R.; and Reinmann, John J.: Steady-State Hot-Ion Plasma Produced by Crossed Electric and Magnetic Fields. NASA TM X-2783, 1973.

3. Sigman, Donald R.; Reinmann, John J.; and Lauver, Milton R.: Parametric Study of Ion Heating in a Burnout Device (HIP-1). NASA TM X-3033, 1974.

4. Thermonuclear Division Annual Progress Report for Period Ending December 31, 1971. ORNL-4793, Oak Ridge National Lab., 1972, p. 33.

5. Hirose, A.; and Alexeff, I.: Nuclear Fusion, vol. 12, no. 3, May 1972, pp. 315-323.

6. Reinmann, J. J.; et al.: Hot Ion Plasma Heating Experiments in SUMMA. IEEE Trans. Plasma Sci., vol. PS-3, no. 1, Mar. 1975, pp. 6-14.

7. Reinmann, J. J.; et al.: NASA Superconducting Magnetic Mirror Facility. Fifth Symposium on Engineering Problems of Fusion Research, Inst. Electrical and Electronics Engrs., Inc., 1974, pp. 587-591.

8. Reinmann, J. J.; et al.: Steady-State Plasma Heating Experiments in SUMMA. Bull. Am. Phys. Soc., vol. 19, no. 9, Oct. 1974, pp. 874, Abst. 2D16.

9. Patch, R. W.; et al.: Ion and Electron Temperatures in the SUMMA Mirror Device by Emission Spectroscopy. NASA TM X-71635, 1974. (See also Bull. Am. Phys. Soc., vol. 19, no. 9, Oct. 1974, p. 975, Abst. 8G2.)

TABLE I. - DATA USED FOR CORRELATIONS

Axial spacing, d + 7.6, cm	Hydrogen flow, G, $\frac{\text{std cm}^3}{\text{sec}}$	Anode-cathode voltage, V, kV	Magnetic flux density, B, tesla	Anode-cathode current, I, A	Ion temperature, T_i, eV	Density product of H^+ ions and H_2 neutrals, $\bar{n}_o \bar{n}_i$
7.6	0.348	16	1.08	0.50	500	10.8
	.354	18	↓	.60	640	9.6
	.358	19		.62	690	9.5
	.363	20		.68	770	8.8
	.363	21		.72	860	8.2
	.373	22		.79	900	8.0
10.2	0.391	16	1.08	0.29	440	4.3
		18	↓	.27	450	3.0
		19		.31	500	2.4
		20		.28	550	1.8
		21		.27	570	1.5
		22		.29	600	1.4
12.7	0.448	10	1.09	0.32	200	26.9
		12	↓	.39	310	14.5
		15		.44	380	9.5
		16		.45	390	8.3
		17		.45	515	5.5
		18		.41	510	4.2
		19		.38	560	3.4
		20		.37	560	3.0
	0.444	21	1.09	0.32	560	2.0
	.458	22	1.09	.33	600	1.8
15.2	0.549	12	1.09	0.40	240	29.7
	.549	14	↓	.57	310	19.9
		16		.66	440	12.2
		17		.70	470	10.0
		18		.74	530	10.6
		19		.80	540	10.6
		20		.88	630	10.0
17.8	0.596	10	1.09	0.35	180	39.9
	.594	12	↓	.40	225	28.5
	.592	14		.46	300	17.9
	.590	15		.47	370	11.3
	.588	16		.51	410	10.9
	.584	17		.52	460	8.1
	.580	18		.54	500	7.0
	.573	19		.54	500	7.2
	.569	20		.55	540	6.4
20.3	0.580	14	1.08	0.84	285	41.6
	.578	15	1.08	.84	310	40.0
	.574	20	1.09	.74	530	11.0
22.8	0.544	14	1.09	0.31	255	22.5
		15	↓	.28	265	15.8
		16		.25	260	12.3
		17.1		.21	300	9.3
		18		.20	340	5.3
		19		.20	360	3.7
		20		.21	400	3.9
		21		.23	420	3.4
		22		.25	460	2.8
		23		.25	480	2.6

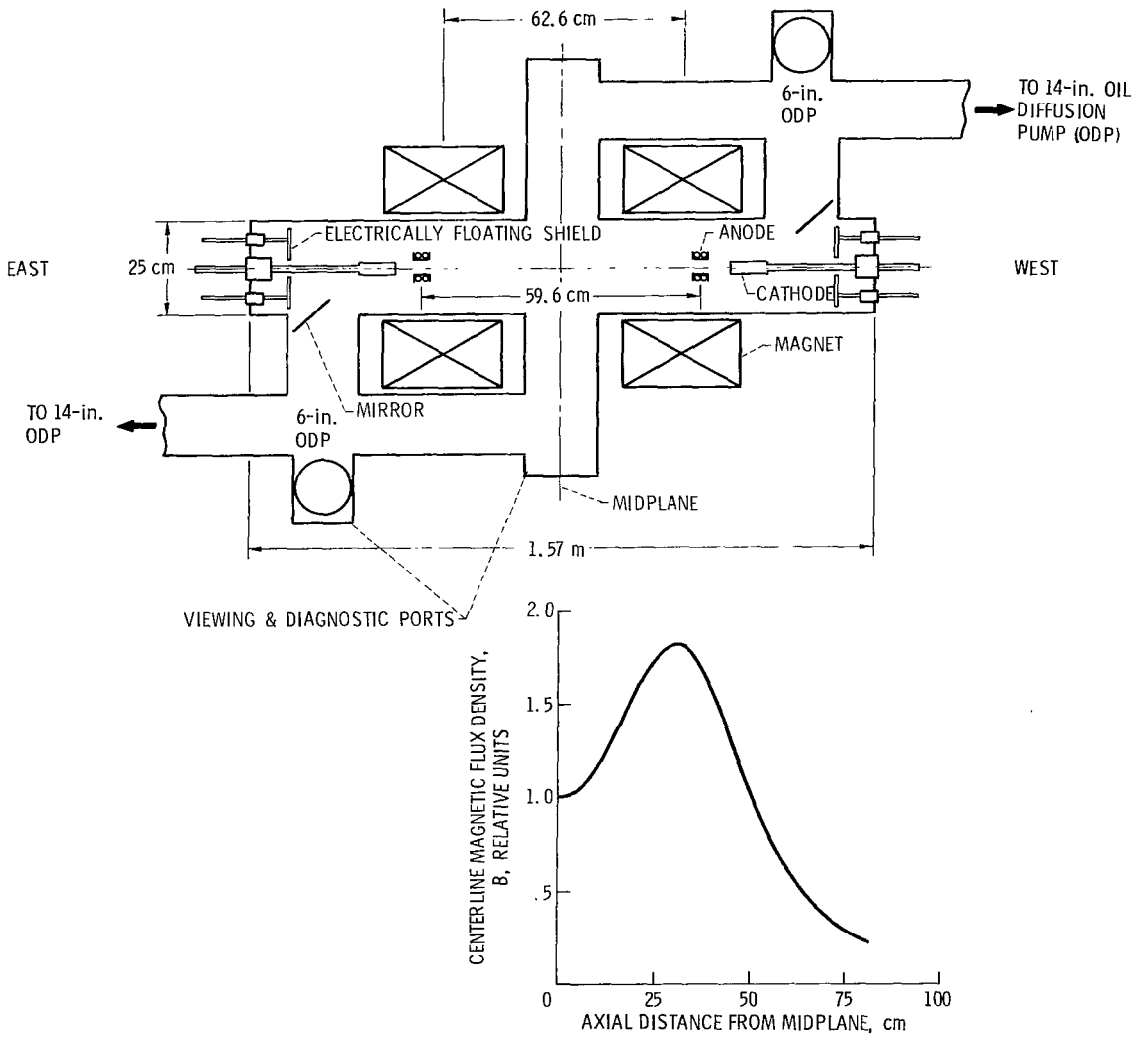

Figure 1. - Test section and magnetic field configuration.

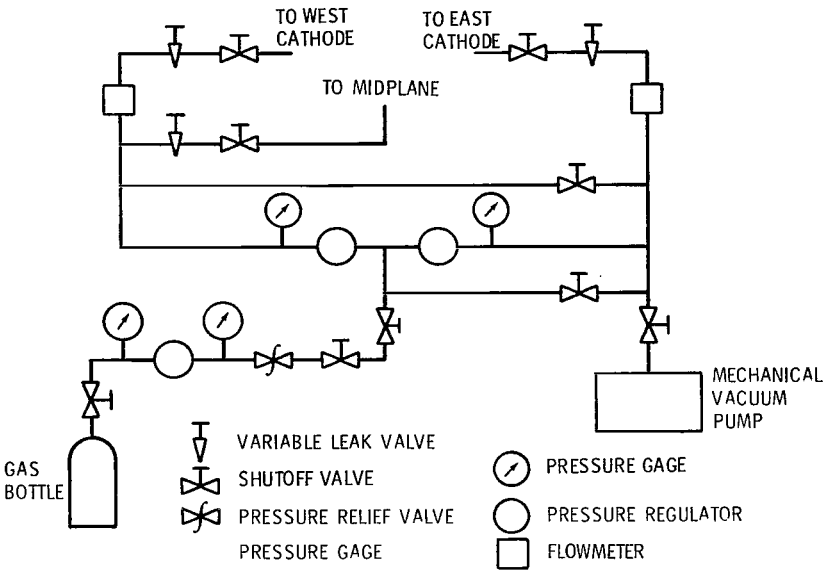

Figure 2. - HIP-1 gas fuel system.

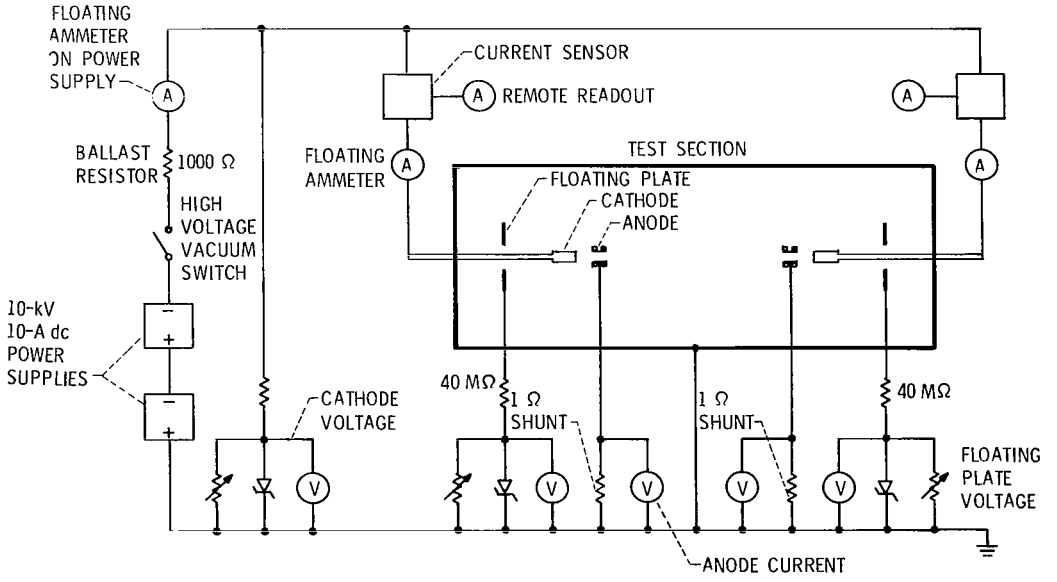

Figure 3. - HIP-1 high voltage schematic.

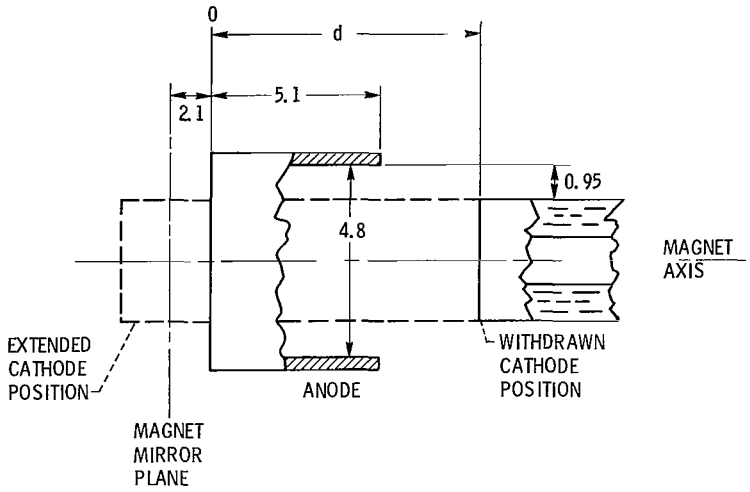

Figure 4. - Electrode nomenclature. (Dimensions in cm.)

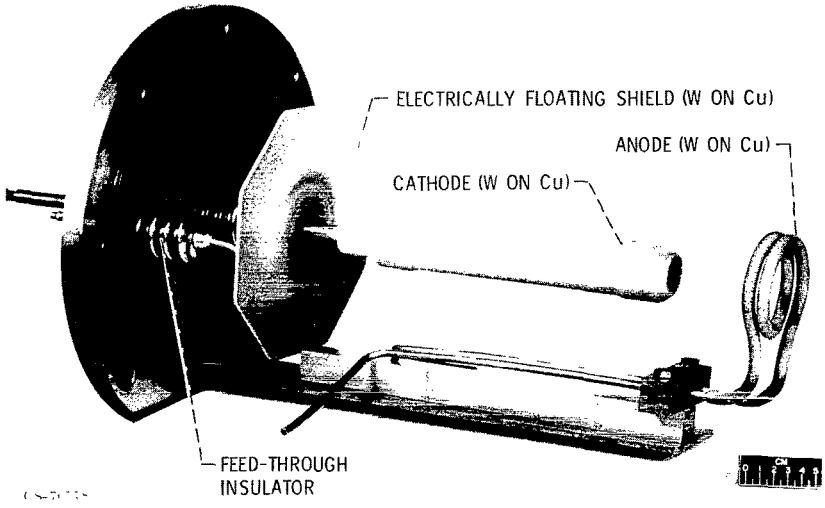

Figure 5. - HIP-1 electrode assembly (typical).

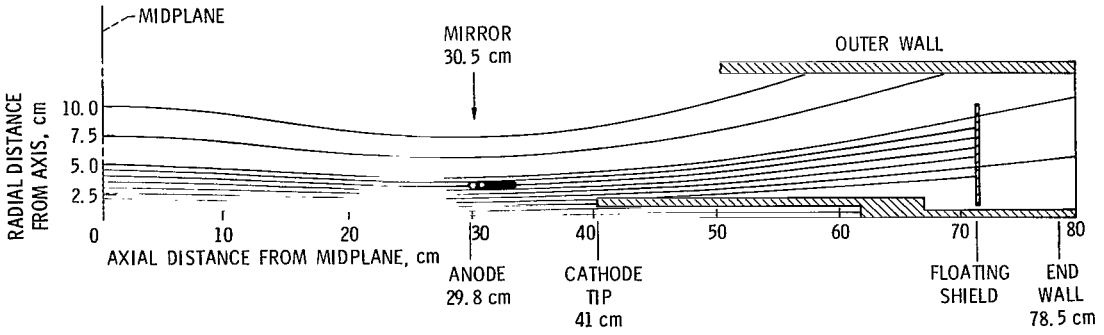

Figure 6. - Magnetic field-line plot showing location of electrodes. Water-cooled cathode.

Figure 7. - HIP-1 water-cooled anodes.

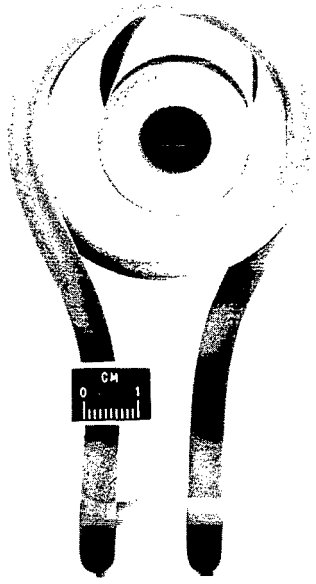

Figure 8. - HIP-1 electrode assembly, view from midplane.

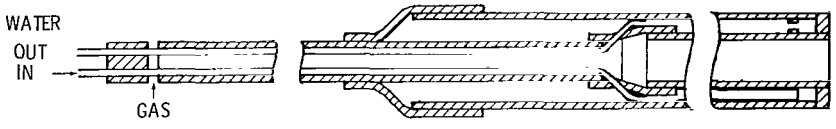

Figure 9. - Cut-away view of water-cooled cathode; inside diameter, 1.3 centimeters; outside diameter, 2.9 centimeters.

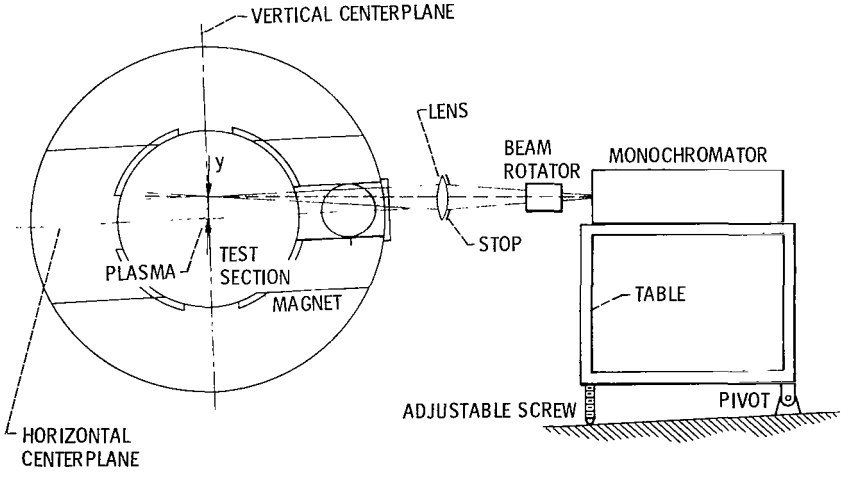

Figure 10. - Apparatus for optical spectroscopic diagnostics. (Not to scale.)

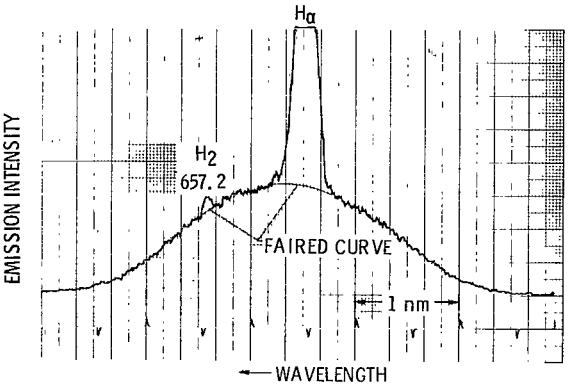

Figure 11. - Typical H_α line exhibiting wide and narrow components.

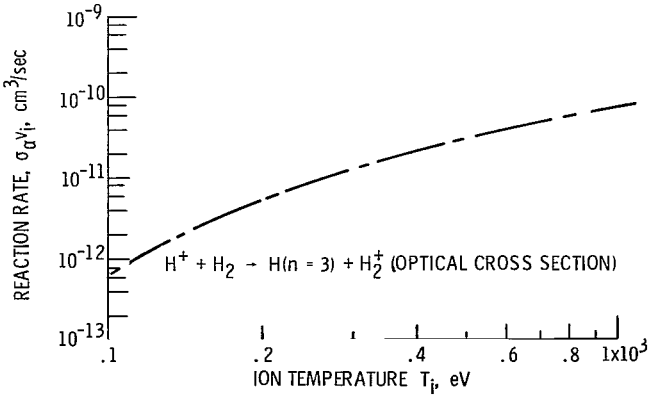

Figure 12. - Maxwell averages for reaction rate.

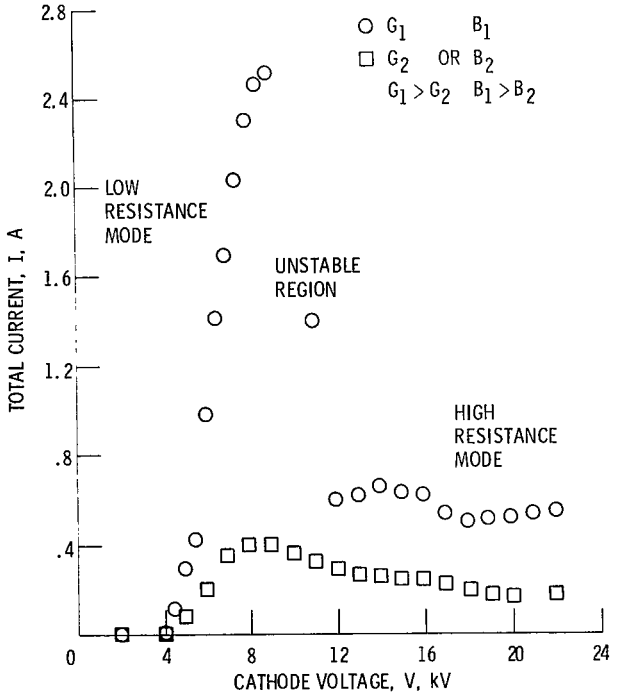

Figure 13. - HIP-1 hot-ion plasma process current-voltage plots for cathode tips positioned at 8.3 centimeters.

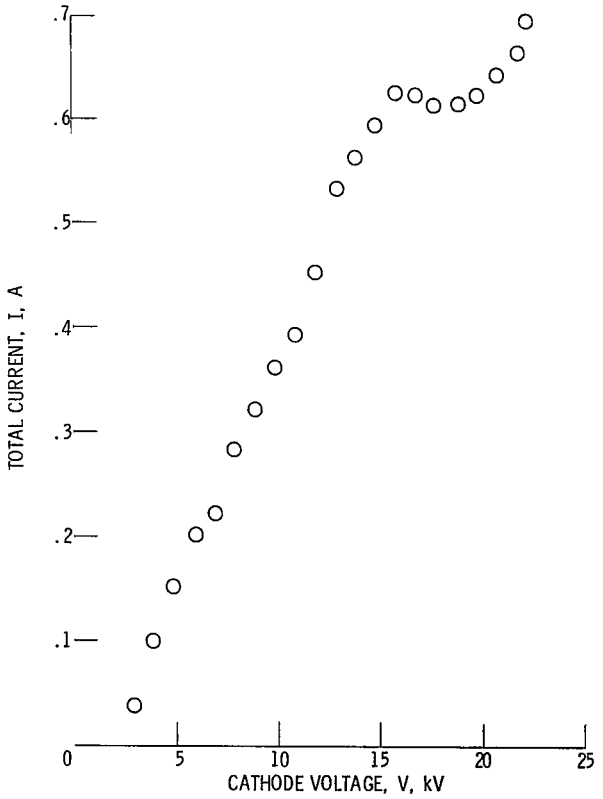

Figure 14. - HIP-1 hot-ion plasma process current-voltage plot for cathode tip positions of 5.1 centimeters or less. Magnetic flux density, 1.02 T; gas flow rate, 0.49 std. cm^3/sec; axial spacing, 5.1 cm.

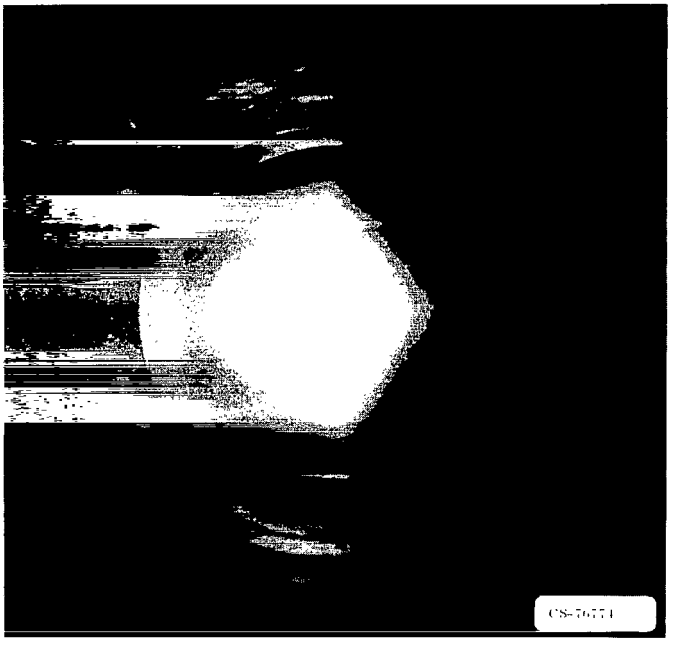

Figure 15. - HIP-1 hydrogen plasma as seen from midplane viewing port.

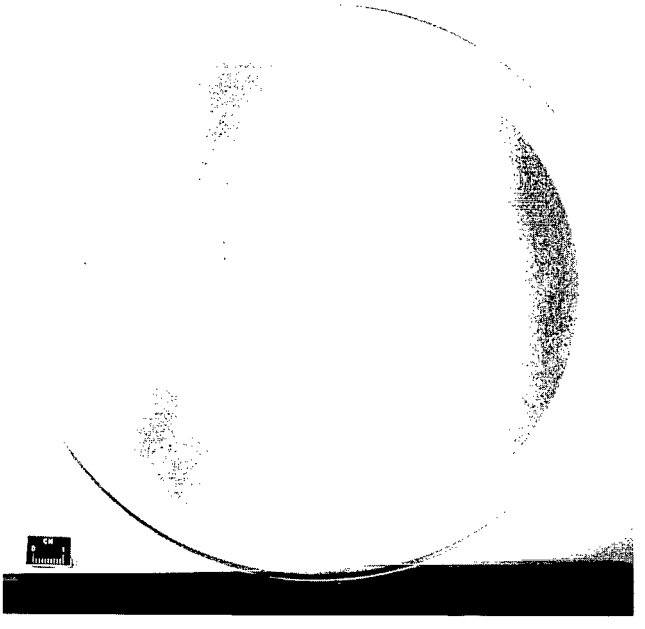

Figure 16. - Midplane window showing deposited metal film and clean area.

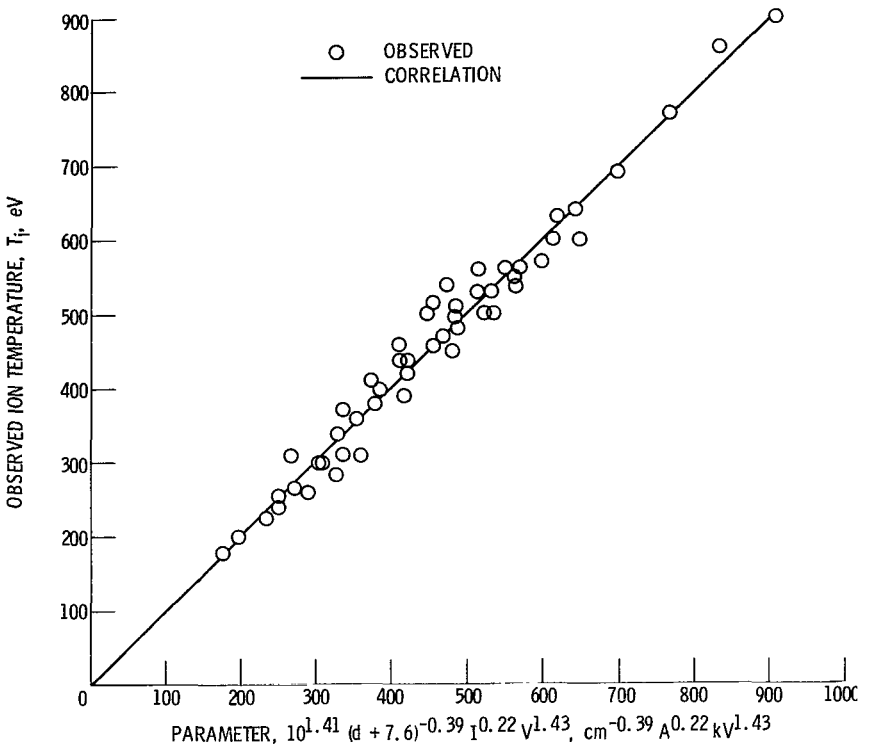

Figure 17. - Correlation of ion temperature.

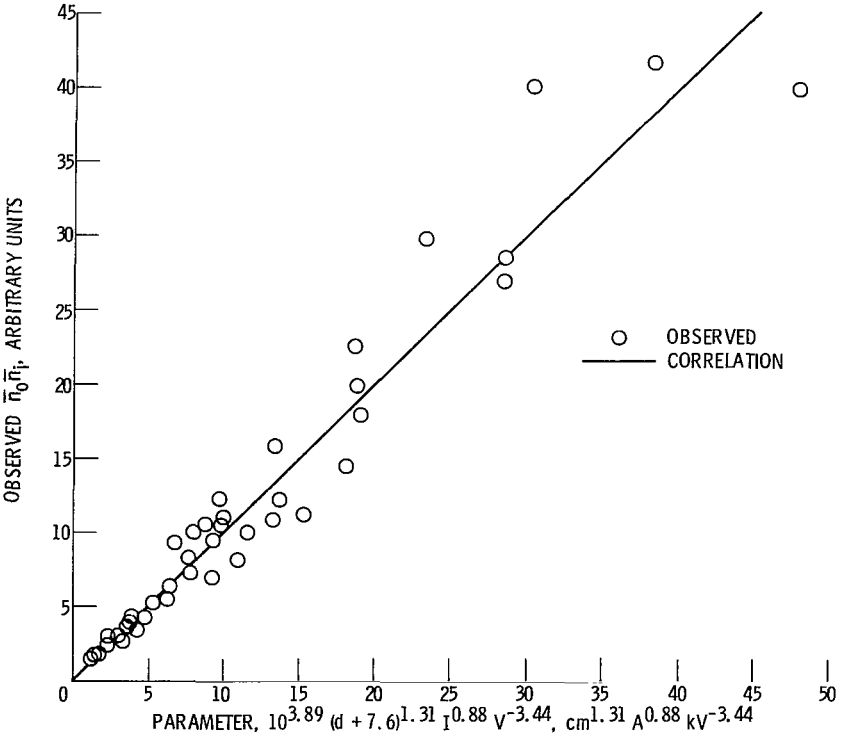

Figure 18. - Correlation of $n_0 n_i$.

1. Report No.	2. Government Accession No.	3. Recipient's Catalog No.
NASA TP-1201		

4. Title and Subtitle	5. Report Date
EFFECT OF ANODE-CATHODE GEOMETRY ON PERFORMANCE OF THE HIP-1 HOT ION PLASMA	April 1978
	6. Performing Organization Code
7. Author(s)	8. Performing Organization Report No.
Milton R. Lauver	E-9386
	10. Work Unit No.
9. Performing Organization Name and Address	506-25
National Aeronautics and Space Administration Lewis Research Center Cleveland, Ohio 44135	11. Contract or Grant No.
	13. Type of Report and Period Covered
12. Sponsoring Agency Name and Address	Technical Paper
National Aeronautics and Space Administration Washington, D. C. 20546	14. Sponsoring Agency Code

15. Supplementary Notes

16. Abstract

Additional results of hot-ion hydrogen plasma experiments conducted in the NASA Lewis HIP-1 magnetic mirror facility are presented. A steady-state E×B plasma was formed by applying a strong radially inward dc electric field near the throats of the magnetic mirrors. The dc electric field was created between hollow cathode rods inside hollow anode cylinders, both concentric with the magnetic axis. The purpose of these experiments was to determine how the ion temperature was influenced by the axial position of the cathode tips relative to the anodes. The highest ion temperatures, 900 eV, were attained when the tip of each cathode was in the same plane as the end of its anode. These temperatures were reached with 22 kV applied to the electrodes in a field of 1.1 tesla. Scaling relations were empirically determined for ion temperature and the product of ion density and neutral particle density as a function of cathode voltage, discharge current, and electrode positions. Plasma discharge current vs voltage (I-V) characteristics were determined.

17. Key Words (Suggested by Author(s))	18. Distribution Statement
Plasma electrodes Ion temperature	Unclassified - unlimited STAR Category 75

19. Security Classif. (of this report)	20. Security Classif. (of this page)	21. No. of Pages	22. Price*
Unclassified	Unclassified	23	A02

* For sale by the National Technical Information Service, Springfield, Virginia 22161

NASA-Langley, 1978

10 1 1U,D, 042078 S00903DS
DEPT OF THE AIR FORCE
AF WEAPONS LABORATORY
ATTN: TECHNICAL LIBRARY (SUL)
KIRTLAND AFB NM 87117